Chaotic advection and transport in helical Beltrami flows: A Hamiltonian system with anomalous diffusion

O. Agullo and A. D. Verga*
Institut de Recherche sur les Phénomènes Hors Equilibre,† 12, avenue Général Leclerc, F-13003 Marseille Cedex, France

G. M. Zaslavsky
Courant Institute of Mathematical Sciences and Department of Physics, New York University, New York, New York 10012
(Received 8 October 1996; revised manuscript received 17 January 1997)

The chaotic advection of a passive scalar in a three-dimensional flow is investigated. The stationary velocity field of the incompressible fluid possesses a helical symmetry and satisfies the Beltrami property, and is then an exact solution to the Euler equations. The streamlines of the fluid form a stochastic web which determines the transport properties. In this cylindrical geometry the origin plays a special role. For pure $2\pi/n$ symmetry (n is an integer) the particles can return to the origin in finite time, as can be demonstrated analytically. The statistical behavior of the passive scalar is studied by using numerical integrations of the motion equations. Subdiffusive behavior is found, the radial variance growing in time with a characteristic exponent of ≈ 0.52 (this exponent is 1 for normal Brownian diffusion). The return probability is also computed. A random walk model, assuming absorption and waiting times proportional to the distance from the origin, appropriately describes the observed features of the particle statistics. In the continuous limit this model gives a diffusion equation with memory effects, highlighting the non-Markovian character of the dynamical system. [S1063-651X(97)08605-4]

PACS number(s): 47.52.+j, 47.27.Qb, 05.40.+j

I. INTRODUCTION

The advection in a fluid, that is, the motion of passive particles which essentially follow the fluid streamlines (they are not relevant in determining the flow velocity), as pollutants which disseminate in the atmosphere, or colorants mixing in water, can be studied from a statistical point of view, assuming, for instance, some *a priori* probability distribution of the velocity field or, alternatively, from a dynamical system point of view, using the concept of chaos of the velocity streamlines. The dynamical system approach leads to the notion of ''Lagrangian turbulence;'' the streamlines associated with a laminar velocity field may be stochastic, filling a dense region of space. In this case the transport properties are inferred *a posteriori*, directly from the properties of the particle trajectories.

The transport of a passive scalar in a stationary three-dimensional (3D) flow, where the given velocity field satisfies Euler equations of an incompressible fluid, is largely an open problem. Indeed, since the pioneering work by Hénon [1] on the Arnold-Beltrami-Childress (ABC) flow [2], which can be considered the starting point of the modern dynamical system approach, it is known that the streamlines of laminar velocity fields can have a complicated topology and densely fill a 3D region. The stochasticity of streamlines drastically modifies the transport properties of the flow; the particles, being frozen, diffuse following the streamlines. Chaotic advection was mostly studied for two-dimensional unstationary flows using the notions issued from the theory of Hamiltonian dynamical systems [3–5]; see [6] for a review. Three-dimensional flow received much less attention, in part because the mathematical theory of the related Hamiltonian system is more complicated [7]. An exception is the study of the *ABC* flow and its relation to the dynamo effect [8], and the quasisymmetric steady state flows investigated by Zaslavsky *et al.* [9,10].

In this paper we analyze the chaotic properties of the streamlines associated with a helical Beltrami flow proposed in [9]. The interest in Beltrami flows is multiple: they are exact, stationary solutions of Euler equations, and are characterized by a vorticity proportional to the velocity, then having a nonvanishing helicity. This property of nonvanishing helicity is essential in order to have a nontrivial topology of the streamlines; otherwise, the existence of an additional constant of motion (resulting from the Bernoulli theorem) ensures the integrability of the Hamiltonian equation of motion of the advected particle. Moreover, they are analogous to the force-free magnetic field configurations often encountered in magnetohydrodynamical problems. In particular, they are relevant for modeling the generation of a magnetic field, the fast dynamo effect, from a dynamical point of view. Finally, Beltrami flows satisfy a variational principle such that the energy is extremal for a given value of the helicity, and then are thought to be relevant configurations even in a turbulent state [11].

One important property of quasisymmetric velocity fields, forming a stochastic web, is their variety of diffusion regimes, which are not limited to the normal diffusion of a Brownian motion [12,13]. Subdiffusive and supradiffusive behavior is also found for the transport of a passive scalar in complex velocity fields, as, for instance, in 2D turbulence where coherent structures dominate the large scales of the

*Electronic address: verga@marius.univ-mrs.fr

†Unité Mixte de Recherche du Centre National de la Recherche Scientifique 138, Universités d'Aix-Marseille I et II.

flow [4,5]. Although the separatrices of the unperturbed stream function (or the associated Hamiltonian) form a complex lattice, no singularities of the velocity field are present. The situation changes in cylindrical geometry, where the origin might become a singular point of the flow. Therefore, the stochastic behavior of the system may depend on the actual region of space explored by the particles, the long time evolution depending on the topology of the streamlines near the origin. This is precisely the situation we study in the present work. Our purpose is to give a phenomenological description of the advection, using numerical simulations, and to explain the salient observed features by analytical developments.

Anomalous diffusion in Hamiltonian systems is the subject of extensive studies. In general, the transport is described by local equations of the Fokker-Planck type [14], where the diffusion coefficient may differ from the quasilinear one [15,16], in this case the standard deviation of the momentum grows as the square root of time (as in the Brownian random walk). In the *ABC* flow and in Beltrami flows, the critical exponents (characterizing the first moments of the particle distribution function) are different from that of the normal diffusion, and were described by a (local) Fokker-Planck equation with fractional derivatives [13]. In this paper we show that non-Markovian effects may also be important, leading to nonlocal (in time) diffusion equations. The inclusion of memory effects allows us to describe the observed anomalous critical exponents.

In Sec. II we state the basic equations defining the flow and particle motion. In Sec. III we describe the stochastic web and analyze the structure of the streamlines near the origin. In Sec. IV, using numerical simulations, we study the statistical and transport properties of the system. A probabilistic model is presented in Sec. V, which assimilates the motion of the particles to a random walk on the stochastic web. Finally, in Sec. VI we present the conclusions.

II. FLUID MODEL AND ADVECTION EQUATIONS

Consider an incompressible and stationary fluid, a solution of the 3D-Euler equations, and denote, respectively, $p,\rho,\mathbf{v}$, the pressure, the density, and the velocity field of the fluid. The Euler equations are written

$$\mathbf{v}\times\boldsymbol{\omega}=\boldsymbol{\nabla}\Phi, \tag{2.1}$$

where $\boldsymbol{\omega}=\boldsymbol{\nabla}\times\mathbf{v}$ is the vorticity, and the potential Φ is defined by

$$\Phi=\frac{p}{\rho}+\frac{v^2}{2}. \tag{2.2}$$

In the spatial regions where $\mathbf{v}\times\boldsymbol{\omega}\neq\mathbf{0}$, it follows that the potential is a first integral of the motion (Bernoulli theorem). Therefore, the streamlines are governed and labeled by their potential values, via Eq. (2.2). If the fluid possesses the Beltrami property, that is, if the vorticity is parallel to the velocity, $\mathbf{v}\|\boldsymbol{\omega}$, the constant of motion degenerates, the potential being constant over all the space, and the streamlines are no longer labeled by Φ. This is the reason by which the Beltrami flows may produce chaotic streamlines, called ''Lagrangian turbulence.'' It is worth noting that the Beltrami condition implies that Eq. (2.1) is an identity which does not give any information on the topology of the streamlines.

A classical way to construct a three-dimensional Beltrami flow is to first search a velocity field depending on only two spatial coordinates, and then to add a ''perturbation,'' including the third coordinates [10]. When the velocity field depends on two coordinates, one can introduce a current function and directly solve a linear partial differential equation for this function (a Hemholtz equation in two dimensions). The perturbation may be added because of the linearity of the Beltrami equation. This perturbation must satisfy the divergence-free condition and the Beltrami constraint. We note that the two-dimensional equations for the velocity streamlines (defined by a constant value of the current function) can be put in Hamiltonian form.

Specific examples of Beltrami flows are the *ABC* flow and the quasiperiodic flows, extensively studied by numerical simulations (see Ref. [10] for an account of the literature on this subject). These systems, where the unperturbed velocity field has a Cartesian geometry, are characterized by a Hamiltonian whose separatrices form a regular lattice in the plane (called a ''web''), invariant by translation in two orthogonal directions of the space. Zaslavski *et al.* [10] introduced a Beltrami flow related to a Hamiltonian system having cylindrical geometry. In the cylindrical geometry the special role played by the origin (symmetry axis of the flow defined by $r=0$) and the nonuniformity of the web can have a significant influence on the properties of the motion of advected particles and their transport.

Let us denote (r,ϕ,z) the cylindrical coordinates of a point in the 3D space. We also introduce the stream function $\psi(r,\phi)$ to describe the basic (unperturbed) two-dimensional flow. The general 3D velocity field $\mathbf{v}=(v_r,v_\phi,v_z)$ of the flow is then defined by

$$v_r=-\frac{1}{r}\frac{\partial\psi}{\partial\phi}+\frac{\epsilon}{r}\sin(z), \tag{2.3a}$$

$$v_\phi=\frac{\partial\psi}{\partial r}-\frac{\epsilon}{r}\cos(z), \tag{2.3b}$$

$$v_z=\psi, \tag{2.3c}$$

where $\psi=\psi(r,\phi)$ satisfies the Helmholtz equation to ensure the Beltrami property

$$\Delta\psi+\psi=0, \tag{2.4}$$

and ϵ, which is an arbitrary parameter, will be considered small in the following. The ϵ terms perturb the basic two-dimensional flow. Units and dimensions were chosen in such a way that the density is $\rho=1$ and the characteristic time and space scales are unity. It is worth noting that this flow is periodic in z, the velocity field being a function of $\sin(z)$ and $\cos(z)$. Moreover, it is easy to verify that, with the perturbation chosen in this way, the Beltrami condition is valid for the whole 3D flow, with the vorticity proportional to the velocity $\boldsymbol{\omega}=-\mathbf{v}$. When $\epsilon=0$, the system is completely integrable, ψ (and then v_z) becomes in this case a constant of motion. The set of equations for the streamlines can be written in Hamiltonian form,

$$\frac{dr}{dz}=\frac{1}{\psi}\left(-\frac{1}{r}\frac{\partial H}{\partial \phi}\right), \tag{2.5a}$$

$$r\frac{d\phi}{dz}=\frac{1}{\psi}\frac{\partial H}{\partial r}, \tag{2.5b}$$

where

$$H=\psi(r,\phi)-\epsilon[\phi\ \sin(z)+\ln(r)\cos(z)]. \tag{2.6}$$

The solution of Eq. (2.4) is the function

$$\psi(r,\phi)=\sum_n C_n J_n(r)\cos(n\phi), \tag{2.7}$$

where C_n are constant coefficients normally determined by boundary conditions, and $J_n(r)$ design the Bessel functions of order n. This gives a multipolar expansion of the velocity field. It is interesting to reduce the study to particular helical flows with a given rotational symmetry. This is done by retaining only one term of the multipolar expansion. Indeed, as will become clear later, when the system is slightly perturbed, because of the geometry of the separatrices of the basic 2D flow having a rotational symmetry, a radial transport having interesting statistical properties may be observed. In this respect, the particular choice of a term in the sum (2.7) is not relevant if the discrete circular symmetry is conserved. Therefore, we retain only the term corresponding to $n=3$ in Eq. (2.7), which possess a rotational symmetry in the plane $z=$const, by the angle $2\pi/3$,

$$\psi=J_3(r)\cos(3\phi). \tag{2.8}$$

The motion of an advected particle in such a flow is, by definition, given by

$$\frac{d\mathbf{r}}{dt}=\mathbf{v}(\mathbf{r}), \tag{2.9}$$

where $\mathbf{r}$ designates the position of the particle, this means that the motion of the particle is uniquely determined by the fluid velocity. When ϵ is zero, the projection of the trajectory of the particle, on the plane (r,ϕ), follows a line of level of the stream function, while its axial velocity is constant and equal to ψ. The lines of level are represented in Fig. 1. A straightforward computation shows that the separatrices associated with ψ are the level lines defined by

$$\psi(r,\phi)=J_3(r)\cos(3\phi)=0. \tag{2.10}$$

They correspond to the lines of Fig. 1 possessing intersections. The intersections of separatrices are the hyperbolic points of ψ. We observe that the separatrices form a regular web and delimit cells. The center of any cell is an elliptic point. In a pair of neighboring cells, the flow is rotating in opposite directions. The points on the symmetry axis are all fixed points of the 2D flow and, of course, a particle initially located at the axis, can never leave it. This is no longer the case when the perturbation is added. When $\epsilon\neq 0$ the advection becomes stochastic due to the destruction of separatrices.

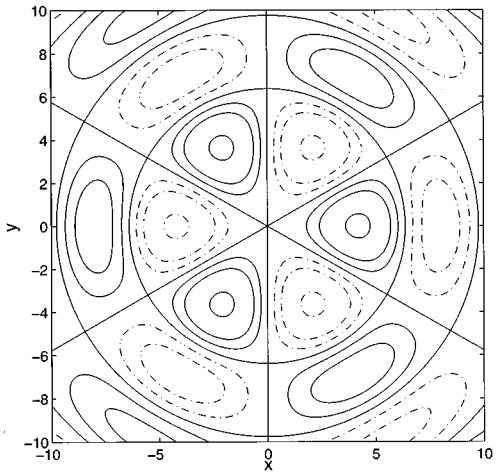

FIG. 1. Contour levels of the stream function ψ in Cartesian coordinates (x,y) showing the web of separatrices and some periodic orbits.

III. STOCHASTIC LAYER AND RETURN TO THE ORIGIN

Let us recall the form of the Hamiltonian system,

$$H=H_0(r,\phi)+\epsilon H_1(r,\phi,z), \tag{3.1}$$

where $H_0=\psi$ is the integrable part of the Hamiltonian. The separatrices of H_0 [see Eq. (2.10)] are defined in the plane by $J_3(r_n)=0$, $n=1,2,\ldots$, which are circles of radius r_n, and radial lines $\phi=(2k+1)\pi/6$, $k=1,2,\ldots$. In destroying the separatrices of H_0, the perturbation ϵH_1 forms stochastic layers for any value of the small parameter ϵ. The structure of the stochastic layer has been thoroughly studied for ''normal'' Hamiltonians, having a kinetic energy term [17]. In the present system, where the phase space is directly the configuration space, the situation is different because the characteristic time scale associated with $z(t)$ is itself determined by H_0. Instead of an exponentially thin stochastic layer (as, for example, for the perturbed pendulum), here the width is at least proportional to ϵ [9] (neglecting logarithmic terms).

The structure of the stochastic layer is illustrated in Fig. 2, by a Poincaré section of the advected particle positions. We compute, using Eqs. (2.9) and (2.3), the trajectories of $N=2048$ particles, initially put around the symmetry axis (and, therefore, near the separatrices), during $t=25\,000$ time units, and a value of $\epsilon=0.2$. Each time a particle crosses the plane $z=0\ (\mathrm{mod}\ 2\pi)$, we plot its position. We observe that they are no longer trapped around the center (as would be the case if ϵ were equal to zero) and they wrap the surfaces generated by $J_3(r)=0$ (cylinders) and $\cos(3\phi)=0$ (half-planes) in the space (r,ϕ,z); that is to say, that stochastic layers are developed around the separatrices of H_0. These separatrices being topologically connected, the stochastic layers are also connected and form the stochastic web shown in the figure. It can be noted that the angular distance between stochastic layers belonging to the separatrices $\phi=$const increases with the radial distance. This is a numerical artifact due to a poor number of particle crossings in these regions, not large enough to fulfill the layers.

To make clear how the advected particles cross the separatrices, we follow one trajectory and plot its projection on

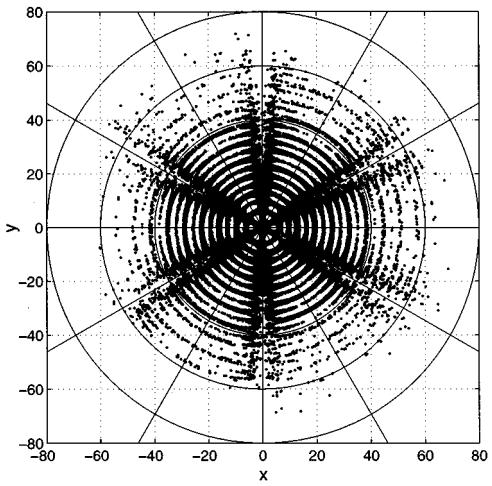

FIG. 2. Poincaré section $z=0 \bmod 2\pi$, of $N=2048$ particles initially at the origin $r(0)=0$, showing the structure of the stochastic layers. Circles of radius 40, 60, and 80 as well as radial lines with angle $2k\pi/6$ $(k=0,1,\ldots,5)$ are plotted. Parameters are $\epsilon=0.2$, final time $t_f=25\,000$.

the plane $z=0$ in Fig. 3. We can see, in this figure, that sometimes the particle appears to be trapped in one cell and stays turning in it before escaping and changing to another cell. In Fig. 3 we also show the radial and axial coordinates $r=r(t)$ and $z=z(t)$. When the particle is trapped in a cell, the motion is almost integrable and $\dot{z}$ is nearly constant; in contrast, when the particle is wandering from one cell to another, $\dot{z}$ undergoes drastic changes correlated with the separatrix crossings. The way the particles cross the separatrix strongly depends on its initial position; an arbitrary small perturbation may lead to a completely different long time behavior of the orbit. In this sense, one is tempted to assimilate the successive crossings as random, in which case the trajectory on the web becomes similar to a random walk.

The case of a particle initially located near an elliptic point is trivial as a consequence of the Kolmogorov-Arnold-Moser theorem, which demonstrates the existence of closed surfaces in the neighborhood of these points. For ϵ small enough, the particle orbit is quasiperiodic and confined in a horizontal plane, as if the perturbation were invisible to it. Such a particle can never cross the web. The regions surrounding an elliptic point are said to be quasi-integrable. These regions are themselves separated and delimited by a cell of the web. Of course, when ϵ becomes large enough, the quasi-integrable regions disappear and the web becomes the whole space. This regime is out of the scope of the present paper.

An interesting feature of the system is the possibility, for the particles advected along the web, of being trapped in a finite time on the axis $r=0$. In fact, this behavior is already present in Fig. 3, where the particle started at $r\approx 9.76$ and $\phi\approx 1.57$ and reached the origin after a time $t\approx 12\,265$.

We analyze the evolution of such particles whose trajectories reach at some time, the neighborhood of the axis. More precisely, we want to show that in such a case, if the value of z is sufficiently close to $\pi/2 \pmod{2\pi}$, the particle trajectory collapses in a finite time to the axis $r=0$. Such a behavior is essentially related to the web geometry. In fact,

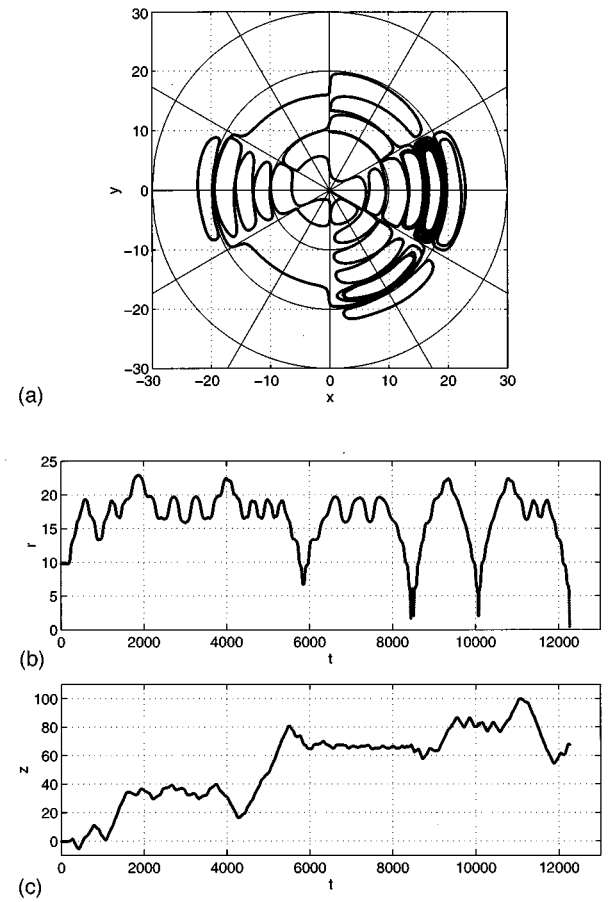

FIG. 3. Trajectory of one particle showing the separatrix crossings. (a) Projection on the plane $z=0$. Circles of radius 10, 20, and 30 as well as radial lines with angle $2k\pi/6$ $(k=0,1,\ldots,5)$ are plotted; (b) radial coordinate as a function of time $r=r(t)$; (c) axial coordinate as a function of time $z=z(t)$. Parameters are $\epsilon=0.2$, $t_f=12\,265$, $r_0=9.76$, and $\phi_0=1.57$.

when the particle falls in the first cylinder (the one generated by the first circular separatrix), following a radial separatrix, it will arrive close to the axis. At this point, according to the value of z, the particle can either go away again taking an ascending radial separatrix or, as we will now show, collapses to $r=0$.

Let us assume that the initial radial position of the particle satisfies (H): $r_0 \ll \epsilon^{1/3}$. Given a set of initial conditions $(r_0,\phi_0,z_0=-\pi/2+u_0)$, with $|u_0|\ll 1$, under the hypothesis (H), we demonstrate that collapse must occur. Indeed, near the origin, the advection equations may be written, using an analytic expansion,

$$16r\dot{r}=[r^3+o(r^3)]\sin(3\phi)-16\epsilon\,\cos u, \tag{3.2a}$$

$$16r^2\dot{\phi}=[r^3+o(r^3)]\cos(3\phi)-16\epsilon\,\sin u, \tag{3.2b}$$

$$48\dot{u}=[r^3+o(r^3)]\cos(3\phi), \tag{3.2c}$$

where we put $z=-\pi/2+u$. Clearly, (H) insures that $\dot{r}_0<0$. Assume the particle returns to the radial position r_0

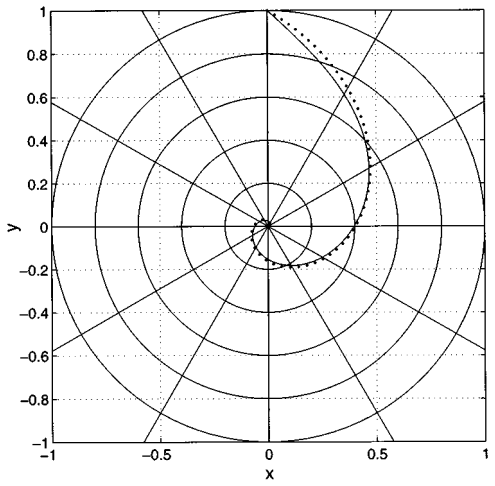

FIG. 4. Collapse on the axis of a particle. Solid line: trajectory of the particle projected on the plane $z=0$ in cylindrical coordinates. The initial conditions are $(r_0,\phi_0,z_0)=(1,\pi/2,\pi-\pi/2+u_0=-\pi/6)$. Circles of radius 0.2, 0.4, 0.6, 0.8, and 1 as well as radial lines with angle $2k\pi/6$ ($k=0,1,\ldots,5$) are plotted. Dashed line: asymptotic computation of the trajectory using $\phi=3^{1/2}\ln(r)+\pi/2$. Parameter is $\epsilon=0.2$.

and let us note $\hat{t}$ ($\hat{t}>0$) the first time the particle reaches it. By definition, as long as t is less than $\hat{t}$, $r(t)$ is less than r_0, and

$$\dot{r}(\hat{t})\geqslant 0. \tag{3.3}$$

Let us define $\tau=(\epsilon\cos u_0)^{-1}r_0^2$, which will appear to be a typical falling time of the particle. Using Eq. (3.2c), we obtain that

$$\forall t\leqslant\hat{t},\quad |u(t)-u_0|\leqslant\frac{r_0^3+o(r_0^3)}{48}t. \tag{3.4}$$

It implies that $\hat{t}\geqslant 2\tau$; otherwise, we would get $|u(\hat{t})-u_0|\ll r_0^2/24\leqslant 1$, and using Eq. (3.2a), we would contradict Eq. (3.3). Equations (3.4) and (3.2a) immediately give,

$$\forall t\leqslant 2\tau,\ \ r(t)\sim a(t)=\sqrt{r_0^2-2\epsilon\cos u_0 t}. \tag{3.5}$$

It is easy to verify that $a(\tau)=0$ and $\dot{a}(\tau)=-\infty$. Therefore, the particle reaches the axis $r=0$ in a finite time (of the order of the falling time τ) with an infinite speed. Of course, the particle never returns to r_0.

The way the particle reaches the axis depends on the initial conditions. If $r_0^3\ll u_0$, the particle spirals down, according to the formulas $\phi=\tan u_0\ln r(t)/r_0+\phi_0$ and $\lim_{r\to 0}r\dot{\phi}=\infty$. This is the case drawn in Fig. 4. If, on the contrary, $r_0^3\gg u_0$, the spiral ends at a particular direction $\phi=\phi(\tau)$.

Besides, it is clear that such a behavior does not depend on the value of n (the order of the symmetry). More generally the hypothesis (H), for general n, would be

$$r_0\ll\epsilon^{1/n},$$

which express the fact that the biggest is n and the weakest is the hypothesis (H) for a given ϵ value.

One may think that the return of the particle to the origin violates the divergence-free condition on the velocity field. To clarify this point, let us consider the 2D radial velocity field

$$\mathbf{v}=-\frac{a}{r}\mathbf{e}_r,$$

which represents, according to the sign of a, the flow generated by a source or a sink. This velocity field is manifestly divergence-free everywhere but at the point $r=0$. In the helical Beltrami flow, the point $r=0$ is replaced by an axis which can be considered alternatively as a sink or a source, according to the values of $\sin(z)$. The physical situation is different in the case of magnetic field lines, although the basic equations $\nabla\cdot\mathbf{B}=0$ and $\nabla\times\mathbf{B}=-\mathbf{B}$ are similar to those satisfied by the velocity field $\mathbf{v}$, because of the inexistence of magnetic monopoles: it is impossible to construct singular sources and sinks of the magnetic field.

IV. RETURN TO ORIGIN STATISTICS

The chaotic nature of the particle trajectories allows us to describe the system at two different levels: a microscopic level, related to the geometrical and dynamical properties of the trajectories themselves which determine the advection properties (fractal dimensions, Lyapunov exponents [6]); and a macroscopic level, related to quantities averaged over a set of trajectories, such as diffusion coefficients or probability distributions of the particle positions, which determine the transport properties of the system. Although the proof of the existence of a probability distribution, and of robust macroscopic quantities from the dynamics, is a difficult problem, only in a few special models can this be done rigorously; a numerical approach is useful in order to investigate the averaged properties of the system. However, it is necessary to test the statistical stability of the macroscopic quantities, for instance, verifying that the macroscopic properties are independent of the details of the particle initial positions.

We showed in the preceding section that the singularity of the flow at the symmetry axis influences the neighboring particles trajectories, leading to collapse in finite time. In particular, one may ask if the long time properties of the transport are also dominated by the cylindrical geometry of the stochastic web, for instance, if the totality of particles are absorbed at the origin (in a finite or infinite time). In order to characterize the role of this singularity on the transport, we define the probability $F(t;\epsilon)$, for a particle starting at the origin, not to be returned before a given time t. This quantity is directly obtained numerically by computing the number of particles $N(t)$ present in the system at time t with respect to the total number of particles N [when this number is large enough, $N(t)/N\to F$].

A distribution of particles is initially given around $r=0$ and $\sin(z)=+1$, where the flow is essentially of the source type. Then, the trajectories are followed, and if a given particle reaches the origin (a sink in the symmetry axis), its return time is computed. The advantage of initializing the system in such a way is that the long time evolution is inde-

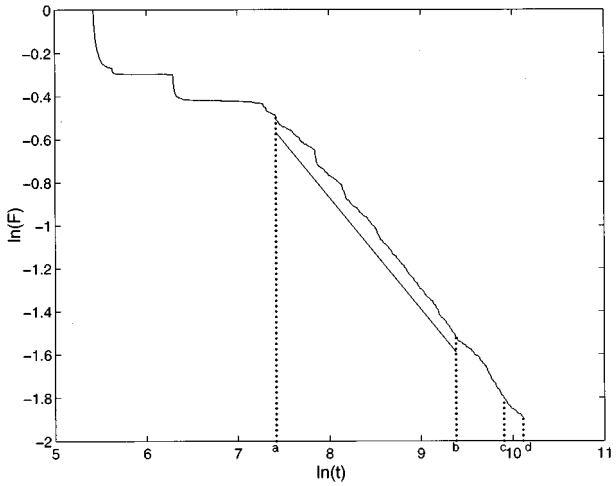

FIG. 5. Temporal evolution of the return probability distribution in logarithmic scales. The average slope of the curve in the intermediate regime, $1664 \leqslant t \leqslant 11\,900$ (between the vertical lines a and b), is -0.52 and is represented by the straight line in the plot. For times $20\,000 \leqslant t \leqslant 25\,000$ (between the vertical lines c and d), the slope is about -0.40. Parameters are $\epsilon = 0.2$, $N = 2048$, $t_f = 25\,000$.

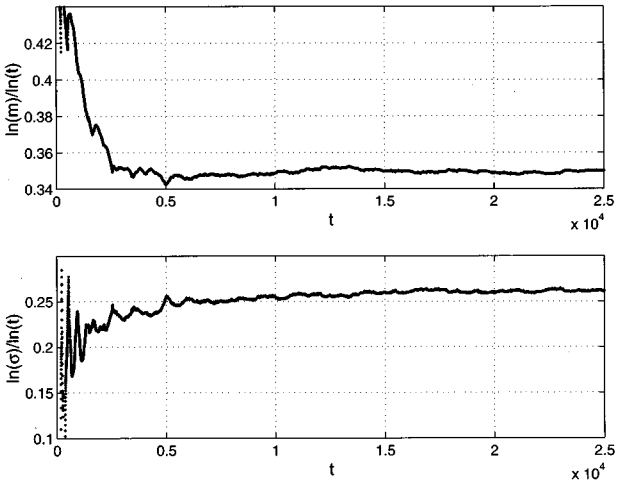

FIG. 6. Temporal evolution of the radial mean (top) and standard deviation (bottom) of the Beltrami flow. Top: $\ln(m)/\ln(t)$ as a function of time. Bottom: $\ln(\sigma)/\ln(t)$ as a function of time. Parameters are $\epsilon = 0.2$, $N = 2048$, $t_f = 25\,000$.

pendent of the initial state and the return to the origin process is properly characterized. This would not be the case if the particles were started, for example, near the first circular separatrix. In such a case it is difficult to define a stable statistical quantity describing the process of concentration near the origin, which may depend on the initial distance.

In Fig. 5 we show the fraction of particles $F(t)$ not returned to the origin as a function of time in a log-log plot, computed from 2048 trajectories and $\epsilon = 0.2$. We observe that, initially, $F(t)$ is like a staircase function: due to the strong correlation of neighboring particle trajectories, these particles reach the origin in clusters. At later times ($t > 1664$), the function $F(t)$ becomes smoother, and slowly decreases from $F(1664) \approx 0.39$, to a value of F equal to 0.15 at the final computed time ($t = 25\,000$). For intermediate times ($1664 < t < 11\,900$) $F(t) \sim t^{-0.52}$ up to the fluctuations and the system behaves almost as a Brownian motion with $F(t) \sim t^{-1/2}$. This may be explained by the fact that the particles explored essentially the origin neighborhood, and long time effects depending on the global geometry of the web cannot yet be manifested. At later times, a change of regime appears, and we observe that the slope of the curve in Fig. 5 tends to decrease. In the range $20\,000 < t < 25\,000$, the average exponent is about 0.40. The long time behavior of $F(t)$ deviates from a Brownian law, but due to the small number of particles remaining at such later times, the statistics become unreliable in determining the behavior. We note that $F(t)$ monotonically decreases, but no asymptotic value strictly larger than zero is reached. If this were the case we would conclude that a fraction of particles may escape from the axis of symmetry, but the numerical simulations are not able to provide an answer to this question.

We verified numerically that ϵ plays, in fact, the role of a normalization time parameter. An appropriate scaling of the time axis in the form $t \to g(\epsilon)t$ lets the distribution probability $F(t)$ be invariant ($F(t;\epsilon) = F[g(\epsilon)t]$, where g is a decreasing function of ϵ). Since the particle transport scaling properties are essentially determined by the topological structure of the web, this behavior demonstrates at least in a statistical sense that the stochastic web topology is fixed by the condition $\epsilon > 0$. This behavior is similar to the transport in Hamiltonian systems [17,16], for example, in the standard map, where the diffusion law is the same for different values of the stochastic parameter, and only the diffusion coefficient depends on the strength of the perturbation.

The departure from the normal Brownian motion may be further investigated using the long time behavior of the mean radial position $m(t)$ and its standard deviation $\sigma(t)$. Moreover, these quantities, which are the first two moments of the radial probability distribution, describe the dispersion of an initially concentrated population of particles near the axis, and, in particular, their asymptotics may account for the possibility of escaping. The mean and standard deviations for a system with absorption at the origin are defined by

$$m(t) = \frac{1}{N(t)} \sum_{p=1}^{N(t)} r_p(t), \tag{4.1}$$

$$\sigma^2(t) = \frac{1}{N(t)} \sum_{p=1}^{N(t)} [r_p^2(t) - m^2(t)], \tag{4.2}$$

where $r_p(t)$ is the radial position of the pth particle at time t not returned to the origin. In this way $m(t)$ and $\sigma(t)$ reflect the actual particle diffusion, and the measure is not biased by the growing number of particles absorbed at $r = 0$.

We used the same kind of initial conditions to measure $m(t)$ and $\sigma(t)$ as we do for measuring $F(t)$. After a short transitory regime, an asymptotic regime sets in, with stable statistical properties. We observe in Fig. 6, where $\ln(m)/\ln(t)$ and $\ln(\sigma)/\ln(t)$ are plotted as functions of t to determine the exponents, that the radial mean and standard deviations follow power laws at long times with exponents about 1/3 and 1/4, respectively,

$$m(t)\sim t^{0.35}, \tag{4.3a}$$

$$\sigma(t)\sim t^{0.26}. \tag{4.3b}$$

The temporal evolution of $\sigma(t)$ is almost independent of the actual value of ϵ and $m(t)$ is an increasing function of ϵ. However, asymptotically, the characteristic exponents (0.35 and 0.26) do not depend on ϵ, which is clearly consistent with the scaling property of F.

We observe that the mean exponent is larger than the standard deviation exponent, suggesting that the distribution of particles is advected far from the origin while slowly spreading. The relative small standard deviation exponent, small with respect to the normal diffusion and also to the radial mean exponent, can be mainly related to two effects. First, the absorption of particles at the origin tends to reduce $\sigma(t)$: some of the particles located far from the mean position disappear, diminishing by way of their dispersion. Second, the radial structure of the separatrices, and the related growth of the cell size with the distance to the origin, contribute to the increase of the circulation time of particles in the farther cells. More precisely, we observe, using the numerical integration of trajectories starting at different distances from the origin, that the particle's time to turn around a cell is proportional to the radial distance of the cell. The proportionality coefficient α typically varies between 1.1 and 1.8, depending on how deep the particle orbit is situated in the cell (see Fig. 3). In a statistical model below, we will take $\alpha=1.4$. The geometry of the web imposes, therefore, a waiting time (the time necessary to turn around one cell) proportional to the distance, whose main effect is to forbid the particles to spread out far from the radial mean (the farther they move, the longer their waiting time is).

V. RANDOM WALK MODEL

We construct a discrete model, based on an average over the z coordinate, of the particle probability distribution. This is justified by the fact that $\dot{z}$ is almost constant on large time scales, so that the radial trajectory is slightly modified by its z value (except when r approaches 0). Therefore, we just consider the projection of the trajectories on the (r,ϕ) plane and we make the approximation that this projection follows the geometry generated by the separatrices of H_0. We obtain a lattice in the plane with lines convergent to the center and concentric circles, the cross points of the separatrices being the hyperbolic points of H_0 (2.10). These hyperbolic points (except for the closest ones from the axis $r=0$) are regularly arranged along the radial axis, the distance between two successive sets of hyperbolic points (of equal radial distance) being approximately constant and equal to π. Therefore, in this model, the radial distance is discrete, the unit distance being the distance between two successive sets of hyperbolic points.

The simplest model that might reproduce the main features of the dynamical system is one where the particles are random walkers on the web, with probability 1/3 of turning left or right or continuing straight on each time they arrive at a hyperbolic point; the time spent going from one hyperbolic point to another one is constant and independent of their position on the web. Let us analyze the radial properties of this model. We assume that a test particle leaves the center of the web and then we compute the probability of the first return to the origin.

It is worth noting that when a particle arrives for the first time at a radial distance r_0 (it turns around the circle of radius r_0), the probability that the particle stays at such a distance for $(i+1)$ steps is $(2/3)^2(1/3)^i$, and the waiting time is

$$\overline{T}=\left(\frac{2}{3}\right)^2\sum_{i=0}^{\infty}(i+1)\left(\frac{1}{3}\right)^i=1. \tag{5.1}$$

Let us denote P_{-+}, the probability of the particle arriving at a hyperbolic point from the bottom moving up, P_{++} the one to move up coming from the top, and similar definitions for P_{+-} and P_{--}. It is easy to verify [18] that the transition matrix probability P is

$$\begin{pmatrix} P_{--} & P_{-+} \\ P_{+-} & P_{++} \end{pmatrix}=\begin{pmatrix} \frac{2}{3} & \frac{1}{3} \\ \frac{1}{3} & \frac{2}{3} \end{pmatrix}, \tag{5.2}$$

and in the limit $n\to\infty$,

$$P^n\approx\frac{1}{2^n}\begin{pmatrix} 1 & 1 \\ 1 & 1 \end{pmatrix}. \tag{5.3}$$

This means that for long times, such a model is, in fact, equivalent to a classical random walk on a line (the radial axis) with an absorbing barrier in $r=0$, a constant waiting time (equal to 1), and a probability 1/2 of going up or down, independently, to the radial position. Therefore, we obtain a radial mean and standard deviation, both increasing asymptotically as $t^{1/2}$. This result is incompatible with the characteristic exponents of the Beltrami flow (4.3).

The main reason this simple model fails is that it does not take into account that the time spent in a cell is approximately, as we already indicated, proportional to the distance of the cell from the center $T=T(r)$. In the frame of a discrete model, T must be an integer number and we take

$$T(r)=E(\alpha r), \tag{5.4}$$

where $E(x)$ denotes the integer part of x and $\alpha\approx1.4$, as we noted before. After this time, the particle can freely leave this position with a given probability.

We denote by $P(r,t|n)$, the conditional probability of a particle being at the radial distance r at time t, knowing that it is there since n time units (the last radial transition was at time $t-n$). Each time a particle is at a transition time, it has probabilities p_-,p_0,p_+ of going up, staying at the same radial position again for a time $T(r)$ [for $p_0=0$ the particle waits exactly $T(r)$ at r], or going down. Time n is therefore a discrete quantity varying from 0 to $T(r)$. Finally, we note, $P(r,t)=P(r,t|0)$ in order to simplify the formulas. In terms of probabilities, the dynamics of the discrete model of the Beltrami flow is defined by

$$\forall r\geqslant 1,1\leqslant n\leqslant T(r),P(r,t|n)=P(r,t-1|n-1), \tag{5.5a}$$

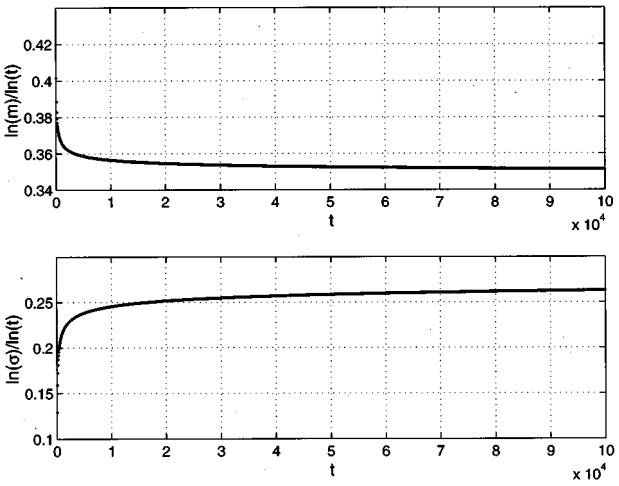

FIG. 7. Temporal evolution of the radial mean (top) and standard deviation (bottom) of the discrete probabilistic model. Top: $\ln(m)/\ln(t)$ as a function of time. Bottom: $\ln(\sigma)/\ln(t)$ as a function of time. Parameters are $(p_+,p_0,p_-)=(0.4,0.2,0.4)$, $\alpha=1.4$, $t_f=100\,000$.

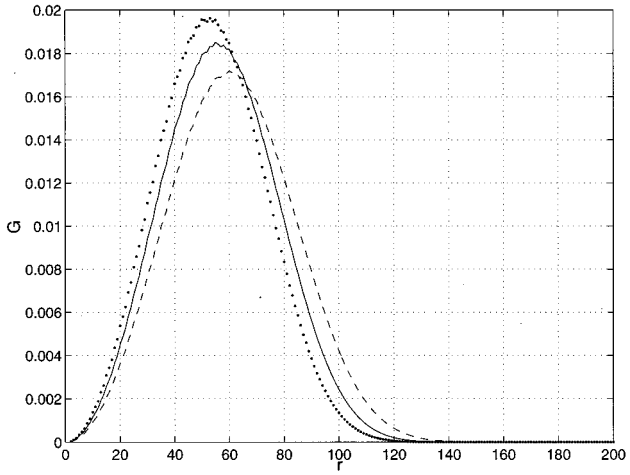

FIG. 8. Radial probability distribution $G(r,t)$ of the discrete model for different values of the waiting transition probability at $t=100\,000$. Dashed line: $p_0=0$; solid line: $p_0=1/5$; and dotted line: $p_0=1/3$. The other transition probabilities are $p_-=p_+$.

$$\forall r\geqslant 2,P(r,t)=p_-P(r-1,t-1|T(r-1)) + p_0P(r,t-1|T(r)) + p_+P(r+1,t-1|T(r+1)), \quad (5.5b)$$

with

$$p_-+p_0+p_+=1, \quad (5.5c)$$

and the absorption condition in $r=0$ (the boundary condition) is given by

$$P(0,t)=p_+P(1,t-1|T(1))+P(0,t-1), \quad (5.5d)$$

$$P(1,t)=p_0P(1,t-1|T(1))+p_+P(2,t-1|T(2)). \quad (5.5e)$$

We can now define $G(r,t)$ the probability for a particle to be at the radial distance r at the time t

$$G(r,t)=\sum_{n=0}^{T(r)}P(r,t|n)=\sum_{n=0}^{T(r)}P(r,t-n). \quad (5.6)$$

The probability normalization condition is written as

$$\forall t\geqslant 0,\sum_{r\geqslant 0}G(r,t)=1. \quad (5.7)$$

To compare with the data of the dynamical system, in the model we concentrate the initial probability distribution around $r=0$ (at $t=0$). The values of p_-, p_0, p_+ chosen are 0.4, 0.2, and 0.4, respectively. The probabilities p_-, p_+ are greater than p_0 to reflect the fact that crossing a circular separatrix is more probable than crossing a radial one, or staying for a long time around the same cell (p_0 makes no distinction between these last two processes, for which the radial position remains the same). The trajectories in the web are essentially composed of radial motions in fixed cones $\theta\in[-\pi/3,\pi/3]+2k\pi/3$, with generally no more than one rotation in each new cell visited. More seldom, the particle is either trapped in a cell or has a change of cone, as is observed in Fig. 3.

To compute the first probability moments (Fig. 7), we do not use the statistics over the particle random walks, but we directly integrate the exact probability distribution evolution, using the algorithm defined by Eqs. (5.5). Although there is no direct relation between the continuous time scale of the system and the discrete one of the model, we can see in Fig. 7 that the characteristic exponents of the mean and the standard deviations are in very good agreement with the values observed in the original dynamical system. The transition of the probabilistic model differs from the one of the Beltrami flow because of its discrete nature, which cannot reproduce the details of the correlations in the absorbing region observed for $t\leqslant 1664$. This results in a smoother convergence to an asymptotic regime. We point out that the approach of the first two moments to this asymptotic regime is similar in both the dynamical and the probabilistic systems.

The model is sensitive to the choice of parameters p_-, p_0, p_+. However, provided that we take p_0 smaller than p_- and p_+, the asymptotics have similar shapes and characteristic exponents. For instance, for $(p_-,p_0,p_+)=(0.5,0,0.5)$, we observe that the exponent of the standard deviation is 0.27 and, at the same time, the exponent of the mean is 0.358. On the other hand, the choice of an equiprobability distribution $(p_-,p_0,p_+)=(1/3,1/3,1/3)$ gives 0.346 and 0.256.

We also computed the return-to-the-origin probability $1-F(t)$ for the discrete model and found the asymptotic behavior $F(t)\sim t^{-1/3}$. This long time power law implies that the probability of a test particle being absorbed in an infinite time, is one. The power law is well defined and extends over many decades in time. This shows, on the other hand, that the numerical simulations had not fully reached the asymptotic regime, even if the first two moments of the probability distribution of particles did.

One interesting point is that the model allows us to compute the exact probability distribution at any time, in contrast to the dynamical system which is limited by the number of

particles not absorbed at the axis. In Fig. 8, the probability distributions are plotted when most of the particles (about 96.5%) are returned to the axis (which corresponds to a time equal to 100 000) for different values of the set (p_-,p_0,p_+). It is logically observed that when increasing p_0, the mean and the standard deviations both decrease. More important, the non-Gaussian nature of the stochastic process appears clearly in the behavior of the probability distribution for large values of r. For a Gaussian process, even with absorption, one expects a decay of the probability as $O[\exp(-ar^2)]$ (the time is fixed); yet we find that for large r the actual probability decays, first, much more slowly than a Gaussian, and then changes progressively to a regime to decay faster than a Gaussian for rare events.

It is interesting to investigate the continuous limit of the discrete model in order to underscore the non-Markovian nature of the stochastic process. We make the simplifying assumption that $(p_-,p_0,p_+)=(1/2,0,1/2)$, taking advantage of the weak dependence on the shape of the probability distribution and on the values of the characteristic exponents of the discrete model. Let us denote τ the unit of time and a the unit of length; in the continuous limit both tend to zero. We define the function

$$f(r,t;a,\tau)=P(r+a,t-\tau-T(r+a))-P(r,t-\tau), \tag{5.8}$$

and with the help of Eqs. (5.5a) and (5.5b), we obtain

$$2[P(r,t)-P(r,t-\tau)]=f(r,t;a,\tau)+f(r,t;-a,\tau). \tag{5.9}$$

In the limit a and τ tending to zero, a Taylor development gives

$$2\tau\frac{\partial}{\partial t}P(r,t)+O(\tau^2)=a^2\frac{\partial^2}{\partial a^2}f(r,t;0,\tau)+O(a^3). \tag{5.10}$$

To get a nontrivial limit, we put $a^2/2\tau=D=\text{const}$ and using (5.8) we obtain

$$\frac{\partial}{\partial t}P(r,t)=D\frac{\partial^2}{\partial r^2}[P(r,t-T(r))], \quad r>0\,. \tag{5.11}$$

We obtain a non-Markovian stochastic process satisfying a nonlocal diffusion equation, with D being the diffusion coefficient, with memory effects depending on the position. It is now straightforward to obtain the continuous limit of Eq. (5.6) and G is then given by

$$G(r,t)=\int_{t-T(r)}^{t}P(r,u)du. \tag{5.12}$$

In fact, P and G are linked by a local relation,

$$\frac{\partial}{\partial t}P(r,t)-D\frac{\partial^2}{\partial r^2}P(r,t)=-D\frac{\partial^3}{\partial r^2\partial t}G(r,t), \quad r>0\,. \tag{5.13}$$

The right hand side of this last equation takes into account the non-Markovian part of the diffusion process and corresponds to the local temporal variation of the diffusion of G. To be complete, we need to add absorption and normalization conditions. We denote $P_0(t)$, the probability of the particle being at $r=0$ at the time t. The absorption condition is written,

$$\frac{d}{dt}P_0(t)=\frac{1}{2}\lim_{r\to 0}G(r,t), \tag{5.14}$$

and the normalization condition becomes

$$P_0(t)+\int_0^{+\infty}G(r,t)dr=1\,. \tag{5.15}$$

We note that the derivation of the continuous equation is independent of the precise form of $T(r)$.

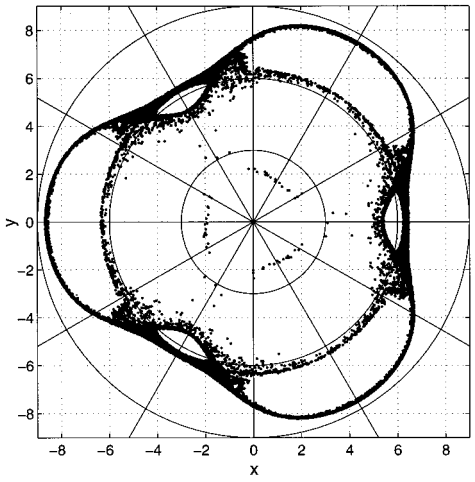

FIG. 9. Poincaré section $z=0 \bmod 2\pi$, of $N=1024$ particles initially located around one separatrix, showing the structure of the stochastic layers for a Beltrami flow having a monopolar contribution with $C_0=1$. Circles of radius 3, 6, and 9 as well as radial lines with angle $2k\pi/6$ $(k=0,1,\ldots,5)$ are plotted. Parameters are $\epsilon=0.1$, final time $t_f=1000$.

VI. CONCLUSIONS

In this paper we studied the advection and transport of test particles in a helical Beltrami flow and showed the stochastic nature of its streamlines. We analytically demonstrate that, under certain conditions, there is a collapse to the origin where the particles may be absorbed. This effect has important consequences in the statistical properties of the system and, in particular, the special topology of the stochastic web determines the behavior of the transport. We introduced several quantities to describe this transport, such as the return probability distribution and the first moments, mean and standard deviations of the radial probability distribution. Numerical integration of the trajectories allowed us to show that the transport is subdiffusive and that the long time behavior of the return probability distribution can be associated with a non-Gaussian random process. In particular, we obtained anomalous exponents for the power laws associated with both the mean and the standard deviations.

In order to verify these results, we proposed a discrete probabilistic model based on a random walk on the separatrix lattice with waiting times proportional to the distance to

the origin. We demonstrated that taking this waiting time constant does not suffice to reproduce the Beltrami flow, and that, in fact, this case reduces to a normal Gaussian process. The model turned out to be, in spite of its relative simplicity, complete enough to explain the observed phenomenology of the transport in the system.

Finally, we derived the continuous limit of the discrete probabilistic model and found that it reduces to a nonlocal diffusion equation with unsteady boundary conditions. This model has interesting properties and can be used as an example of the non-Markovian stochastic process, with the advantage that its discrete version is known and easily computable numerically.

The symmetry we choose for the helical Beltrami flow, with only one Bessel function (in our case the one of order 3), is fundamental in determining the behavior of the system. It is precisely this (discrete) cylindrical symmetry which is essential in the absorption process. To illustrate this point we computed the Poincaré section (Fig. 9) of a helical Beltrami flow having two components: the Bessel of order 3 plus a monopolar contribution (a Bessel of order 0). The monopolar term completely modify the geometry of the stochastic web, in particular, eliminating the separatrices converging toward the origin. One consequence of the topological change is that the transport becomes essentially in the angular direction rather than in the radial one.

ACKNOWLEDGMENTS

We thank X. Leoncini and D. Benisti for useful discussions. Part of this work was carried out at the Equipe Turbulence Plasma. One of us (G.M.Z.) was supported by the U.S. Department of the Navy, Grant No. N00014-96-1-0055, and the U.S. Department of Energy, Grant No. DE-FG02-92ER54184. The numerical computations were performed at the Centre de Calcul Régional of the Institut Méditerranean de Technologie (Région Provence-Alpes-Côte d'Azur).

[1] M. Hénon, C. R. Acad. Sci. **262**, 312 (1966).
[2] V. Arnold, *Les Méthodes Mathématiques de la Mécanique Classique* (Editions Mir, Moscow, 1976).
[3] H. Aref, J. Fluid Mech. **143**, 1 (1984).
[4] D. Elhmädi, A. Provenzale, and A. Babiano, J. Fluid Mech. **257**, 533 (1993).
[5] A. Babiano, G. Boffeta, A. Provenzale, and A. Vulpiani, Phys. Fluids **6**, 2465 (1994).
[6] J.M. Ottino, Annu. Rev. Fluid Mech. **22**, 207 (1990).
[7] S. Wiggins, *Chaotic Transport in Dynamical Systems* (Springer-Verlag, New York, 1992).
[8] D. Galloway and U. Frisch, Geophys. Astrophys. Fluid Dyn. **36**, 53 (1986).
[9] G. M. Zaslavsky, R. Z. Sagdeev, and A. A. Chernikov, Zh. Éksp. Teor. Fiz. **94**, 102 (1988) [Sov. Phys. JETP **67**, 270 (1988)].
[10] G.M. Zaslavsky, R.Z. Sagdeev, D.A. Usikov, and A.A. Chernikov, *Weak Chaos and Quasi-regular Patterns* (Cambridge University Press, Cambridge, England, 1991).
[11] P. Constantin and A. Majda, Commun. Math. Phys. **115**, 435 (1988).
[12] D. K. Chaikovsky and G. M. Zaslavsky, CHAOS **1**, 463 (1991).
[13] G. M. Zaslavsky, Physica D **80**, 341 (1994).
[14] A.J. Lichtenberg, and Liberman, *Regular and Stochastic Motion* (Springer-Verlag, New York, 1983).
[15] A.B. Rechester, M.N. Rosenbluth, and R.B. White, Phys. Rev. Lett. **42**, 1247 (1979).
[16] J.R. Cary, D. Escande, and A.D. Verga, Phys. Rev. Lett. **65**, 3132 (1990).
[17] B.V. Chirikov, Phys. Rep. **52**, 263 (1979).
[18] W. Feller, *Introduction to Probability Theory and its Applications* (Wiley, New York, 1968).